by Assumption 1, we have $s_{ij_0}(t)=0$. Thus $s_{ij_0}(t)=0$ for all $j_0 \in P$. Since

$$w_i(t+1)=w_i(t)=m_1(t)$$

and

$$w_i(t+1)=w_i(t)+\sum_{j\in P} r_{ji}(t),$$

we have $r_{j_0 i}(t)=0$, and this prove (3) for *k=1*. Therefore, (1),(2) and (3) are proved for *k=1*.

In continuation, the induction step on *k* is outlined. Suppose now that *l>1* and that there exists $t_1<t_2<t_3<\ldots<t_{l-1}$ positive integers such that for all *k*, $(1\le k<l)$, (1), (2) and (3) hold.

Let $i\in P\setminus\bigcup_{k=1}^{l-1} P_k(t_k)$. We shall see that

$$w_i(t+1)\ge m_1(t),$$

for all $t\ge t_{1-1}+B$.

Let $t\ge t_{1-1}+B$. If $s_{ij}(t)=0$ for all $j\in P$, then

$$w_i(t+1)=w_i(t)+\sum_{j\in P} r_{ji}(t)\ge w_i(t)\ge m_l(t).$$

If $s_{ij_0}(t)>0$ for some $j_0\in P$, then, as above,

$$w_i(t+1)\ge w_{ij_0}(t)+s_{ij_0}(t)=w_{j_0}(\tau_{ij_0}(t))+s_{ij_0}(t).$$

• Note that: $P\setminus P_1(t)=\overline{P_1(t)}$

Since $r_{ij_0}(t') > 0$ for some $t' > t$, we have

$$j_0 \notin \bigcup_{k=1}^{l-1} P_k(t_k) = \bigcup_{k=1}^{l-1} P_k(t''), \quad \forall t'' \geq t_{l-1}.$$

Since $\tau_{ij_0}(t) > t - B \geq t_{l-1}$,

$w_{j_0}(\tau_{ij_0}(t)) > m_{l-1}(t)$, so $w_{j_0}(\tau_{ij_0}(t)) \geq m_l(t)$.

Thus $w_i(t+1) \geq w_{j_0}(\tau_{ij_0}(t)) + s_{ij_0}(t) > m_l(t)$.

Hence $(m_l(t))_{t \geq t_{l-1}+B}$ is a non-decreasing sequence of integers $\leq L$. Thus there exists an integer $t_l' > t_{l-1}$ such that

$$m_l(t) = m_l(t_l') \quad \forall t \geq t_l'.$$

So (1) follows for *k=1*.

In order to prove (2), we shall see that

$$P_l(t_l') \supseteq P_l(t_l'+1) \supseteq P_l(t_l'+2) \supseteq \ldots \qquad (**)$$

Let $t \geq t_l'$ and let $i \in P \setminus P_l(t)$. If $i \in P_k(t)$ for some $k = 1,\ldots,l-1$, then $i \in P_k(t+1)$, so $i \in P \setminus P_l(t+1)$. Suppose that let $i \in P \setminus \bigcup_{k=1}^{l} P_k(t)$. If $s_{ij}(t) = 0$ for all $j \in P$, then

$$w_i(t+1) \geq w_i(t) > m_l(t) = m_l(t+1).$$

If $s_{ij_0}(t) > 0$ for some $j_0 \in P'$, then, as above,

$$w_i(t+1) > m_l(t) = m_l(t+1).$$

Thus $i \in P \setminus P_l(t+1)$ and this proves (**). Since $P_l(t_l^{'})$ is a finite set, there exists $t_l \geq t_l^{'}$ such that

$$P_l(t) = P_l(t_l) \quad \forall t \geq t_l .$$

So (2) is true for *k=l*.

In order to prove (3), let $t \geq t_l$, let $i \in P_l(t_l)$ and let $j_0 \in P$. If $j_0 \in \bigcup_{k=1}^{l-1} P_k(t_k)$ then $s_{ij_0}(t) = 0$, because $r_{j_0 i}(\tau) = 0$ for all $\tau \geq t_{l-1}$. If $j_0 \in P \setminus \bigcup_{k=1}^{l-1} P_k(t_k)$ then

$$w_i(t) > m_l(t) \leq w_{ij_0}(t),$$

by Assumption 1, we have $s_{ij_0}(t) = 0$. Since $w_i(t+1) = w_i(t) = m_l(t)$ and

$$w_i(t+1) = w_i(t) + \sum_{j \in P} r_{ji}(t)$$

we have $r_{j_0 i}(t) = 0$, and this proves (3) for *k=l*. This concludes the induction step and the proof of the theorem. ■

We have proved the convergence of the proposed realistic IDLB model, however, no consideration concerning the final balance degree has been provided. *Corollary A.1* gives an upper bound for the maximum load difference throughout the whole system when the stable load distribution is achieved. For that purpose, a new assumption is included in the LB model described this section: the maximum load difference in any *t*-domain in the system at the end of the load-balancing process is restricted to being one load unit. Consequently, the final maximum load difference among the system is upper bounded by the diameter of the underlying topology (*d*).

Corollary A.1. *Assume Assumption 1,2 and 3. Let* $t \in T_i$. *Assume that* $\exists j \in D(i,t)$ *such that* $w_i(t) - w_{ij}(t) > 1$ *then* $\exists j' \in D(i,t)$ *with* $w_i(t) - w_{ij'}(t) > 1$ *and* $s_{ij'}(t) \geq 1$. *If* $\bar{t}$ *is as in Theorem A.1, then*

$$\left| w_i(t) - w_j(t) \right| \leq d, \quad \forall i, j \in P, \forall t \geq \bar{t} + B,$$

where d is the diameter of G.

Proof. Note that $\{ j \in P \mid \{i,j\} \in E \} \subseteq D(i,t)$ for all $t \geq 2B$. By (b2) and (c2), we have

$$\left| w_i(t) - w_j(t) \right| \leq 1, \quad \forall \{i,j\} \in E, \forall t \geq \bar{t} + B.$$

Hence

$$\left| w_i(t) - w_j(t) \right| \leq d, \quad \forall i, j \in P, \forall t \geq \bar{t} + B. \blacksquare$$

Appendix B

Comparative study of nearest-neighbour load-balancing algorithms: *complementary tables*

Hypercube (*dif_max*)									
	Number of Proc.	*likely distributions*				*pathological distributions*			
		25%	50%	75%	100%	25%	50%	75%	n-1
D A S U D	8	0.3	0.5	0.6	0.2	0	1	0	2
	16	1	1	1	1	1	1	1	1
	32	1.5	1.5	1.6	1.65	2	1.5	1.5	2
	64	1.75	2	2.2	2	2	2	2	3
	128	1.95	2.15	2.45	2.6	2.5	2	2	3
S I D	8	8.65	8.65	8.9	8.85	3	3	3	6
	16	22	23.4	24,45	25.1	11.5	22.5	19	20
	32	20.65	31.9	36.7	35.85	50.5	39.5	35	50
	64	14	24.45	31.3	38.3	55.5	37.5	38.5	66
	128	8.45	11.45	24.5	29.1	28.5	30	25	46
G D E	8	2.3	2.4	2.5	2.1	2	2.5	2.5	3
	16	2.5	2.6	2.81	2.71	3	2.5	3	3.5
	32	3.1	3.2	3.12	3.4	3.5	3	3.5	3.5
	64	3.7	3.75	3.7	3.84	3.5	4	4	4
	128	3.9	4.05	4.1	4.3	4	4	4	4
A N	8	1.2	0.4	1	0.6	1	0	0	0
	16	1.4	1.2	1.1	1.4	1.5	2	1.5	1
	32	2	1.6	2.1	2.1	1.5	2.5	2.5	2
	64	2.8	3	3.5	3.7	2.5	2.5	2.5	3
	128	3.5	3.7	4	3.9	4	3.5	4	5

Table B.1 Maximum load difference for DASUD, SID, GDE and AN considering likely and pathological initial load distributions for hypercubes attending to the architecture size and initial distribution patterns.

Torus (*dif_max*)									
	Number of Proc.	*likely distributions*				*pathological distributions*			
		25%	50%	75%	100%	25%	50%	75%	n-1
D A S U D	9	0.9	0.8	0.9	0.8	1	1	1	1
	16	1	1	1	1	1	1	1.5	1.5
	36	1	1	1	1	1	1	1	1
	64	2	2	2	2	2	2	2	2
	121	2.8	3.1	3.15	3.15	4	3	4	4
S I D	9	6.75	7.8	9.1	8.75	7	7.5	5.5	4
	16	21.7	23.5	24.55	26.3	11.5	20.5	18	20
	36	20.05	32.05	41.95	43.9	62.5	36	48	73
	64	14	26.5	34.5	43.85	55.5	52.5	49	67
	121	8.95	16.3	23.55	31.25	28	41	43.5	60
G D E	9	1.5	1.6	2	2	2	2	2	2
	16	1.7	2.3	3.1	3	2	2	2.5	2.5
	36	2.45	2.5	3.5	3.25	3	3.5	3.5	3
	64	3.75	3.8	4.7	4.5	4.5	4	4	4
	121	4.7	4.9	4.9	5	4.5	4.5	4.5	4.5
A N	9	1	1.1	1.1	1.1	1	1	1	1
	16	1.2	1.2	1.7	1.5	1	1	1	1
	36	2.4	2.5	2.4	2.2	2	1.5	1.5	3
	64	2.8	3.2	3.1	3.1	3	3.5	3	2
	121	3.9	4.1	4.4	4.6	4	4	4.5	4

Table B.2 Maximum load difference for DASUD. SID. GDE and AN considering likely and pathological initial load distributions for torus attending to the architecture size and initial distribution patterns

Hypercube (*dif_max*)									
	Shape	*likely distributions*				*pathological distributions*			
		25%	50%	75%	100%	25%	50%	75%	n-1
DASUD	SM	1.68	1.76	1.84	1.62	1.6	2	1.8	2.2
	Chain	0.94	1.12	1.34	1.36	1.4	1	0.8	
SID	SM	20.6	30.44	36.82	40.84	35.2	39.6	40.8	37.6
	Chain	8.9	12.04	13.52	35.1	26.4	13.4	9.4	
GDE	SM	3.27	3.31	3.4	3.42	3.8	3.6	3.5	3.7
	Chain	2.9	3.02	3.17	3.2	3.3	3.15	3.3	
AN	SM	2.24	2.12	2.08	2.24	3.34	2.64	2.86	2.88
	Chain	2.12	1.84	2.46	2.24	2.32	2.88	2.9	

Table B.3 Maximum load difference for DASUD, SID, GDE and AN considering likely and pathological initial load distributions for hypercubes attending to the initial distribution patterns and shapes

Torus (*dif_max*)									
	Shape	*likely distributions*				*pathological distributions*			
		25%	50%	75%	100%	25%	50%	75%	n-1
DASUD	SM	1.58	1.64	1.58	1.58	1.8	1.6	1.8	1.8
	Chain	1.5	1.52	1.64	1.6	1.8	1.6	1.8	
SID	SM	19.8	30.96	39.86	45.7	37.8	38.8	47.2	44.8
	Chain	8.84	11.78	13.68	15.94	28	24.2	19.2	
GDE	SM	3.3	3.41	3.3	3.4	3.55	3.42	3.5	3.4
	Chain	3.1	3.11	3.22	3.27	3.47	3.2	3.24	
AN	SM	2.32	2.44	2.46	2.47	2.8	2.4	2.2	2.5
	Chain	2.16	2.36	2.6	2.58	2.4	3	2.4	

Table B.4 Maximum load difference for DASUD, SID, GDE and AN considering likely and pathological initial load distributions for torus attending to the initial distribution patterns and shapes

Hypercube (*standard deviation - σ*)									
	Number of Proc.	*likely distributions*				*pathological distributions*			
		25%	50%	75%	100%	25%	50%	75%	n-1
DASUD	8	0.05	0.025	0	0.05	0	0	0	0
	16	0.5	0.5	0.5	0.5	0.5	0.5	0.5	0.5
	32	0	0	0	0	0	0	0	0
	64	0.01	0.01	0.01	0.01	0.01	0.01	0.01	0.01
	128	0.5	0.5	0.5	0.5	0.5	0.5	0.5	0.5
SID	8	2.45	2.57	2.69	2.6	1.05	0.86	1.06	1.73
	16	5.46	5.8	5.85	5.99	3.1	5.91	4.79	4.8
	32	5.08	6.44	7.15	6.89	9.99	8.22	6.65	8.93
	64	3.73	6.17	7.49	6.16	10.55	7.38	7.98	11.14
	128	2.22	4.57	6.33	7.59	6.94	6.92	7.85	11.7
GDE	8	0.5	0.5	0.5	0.6	0.6	0.6	0.6	0.6
	16	0.6	0.6	0.6	0.7	0.74	0.7	0.7	0.7
	32	0.65	0.6	0.6	0.82	0.81	0.8	0.8	0.83
	64	0.85	0.75	0.8	0.82	0.92	0.8	0.8	0.92
	128	1.3	1.1	1.1	1.1	1.3	1.2	1.2	1.35
AN	8	0.02	0.02	0.015	0.02	0.0	0.0	0.0	0.0
	16	0.2	0.22	0.2	0.25	0.2	0.2	0.22	0.22
	32	0.0	0.0	0.0	0.0	0.0	0.0	0.0	0.0
	64	0.01	0.01	0.01	0.01	0.01	0.01	0.01	0.01
	128	0.25	0.3	0.3	0.3	0.3	0.3	0.3	0.3

Table B.5 Standard deviation for DASUD, SID, GDE and AN considering likely and pathological initial load distributions for hypercubes attending to the architecture size and initial distribution patterns.

Torus (*standard deviation - σ*)									
	Number of Proc.	*likely distributions*				*pathological distributions*			
		25%	50%	75%	100%	25%	50%	75%	n-1
DASUD	9	0.35	0.34	0.35	0.33	0.47	0.47	0.47	0.47
	16	0.5	0.5	0.5	0.5	0.5	0.5	0.5	0.5
	36	0.01	0.01	0.01	0.01	0.01	0.01	0.01	0.01
	64	0.01	0.01	0.01	0.01	0.01	0.01	0.01	0.01
	121	0.69	0.715	0.72	0.73	0.765	0.74	0.73	0.76
SID	9	2.12	2.32	2.75	2.71	2.46	2.33	2.17	1.33
	16	5.39	5.66	5.89	6.18	3.1	5.47	4.47	4.72
	36	5.31	7.14	8.22	8.64	12.69	9.23	10.01	13.26
	64	4.1	7.76	9.52	11.4	14.44	13.84	12.63	16.77
	121	2.57	4.62	6.67	8.9	9.46	13.3	13.16	18.38
GDE	9	0.5	0.5	0.5	0.6	0.6	0.6	0.6	0.6
	16	0.6	0.6	0.6	0.6	0.7	0.7	0.7	0.75
	36	0.75	0.77	0.7	0.75	0.77	0.8	0.8	0.8
	64	0.85	0.82	0.8	0.83	0.97	0.97	0.97	0.97
	121	1.3	1.27	1.3	1.31	1.3	1.3	1.3	1.32
AN	9	0.15	0.16	0.16	0.16	0.18	0.18	0.18	0.2
	16	0.2	0.22	0.2	0.2	0.2	0.2	0.22	0.22
	36	0.01	0.01	0.01	0.01	0.01	0.01	0.01	0.01
	64	0.02	0.02	0.02	0.02	0.01	0.01	0.02	0.01
	121	0.34	0.3	0.4	0.3	0.45	0.45	0.45	0.4

Table B.6 Standard deviation for DASUD. SID. GDE and AN considering likely and pathological initial load distributions for torus attending to the architecture size and initial distribution patterns

Hypercube (*standard deviation - σ*)									
	Shape	*likely distributions*				*pathological distributions*			
		25%	50%	75%	100%	25%	50%	75%	n-1
DASUD	SM	0.2	0.2	0.2	0.2	0.2	0.2	0.2	0.2
	Chain	0.22	0.21	0.2	0.22	0.2	0.2	0.2	
SID	SM	5.29	7.19	8.42	8.84	7.32	8.24	9.03	7.66
	Chain	2.31	3.03	3.38	3.57	5.33	3.47	2.3	
GDE	SM	0.8	0.7	0.75	0.81	0.87	0.8	0.83	0.88
	Chain	0.74	0.7	0.75	0.8	0.86	0.8	0.81	
AN	SM	0.1	0.15	0.11	0.15	0.1	0.15	0.1	0.1
	Chain	0.1	0.1	0.08	0.1	0.1	0.1	0.1	

Table B.7 Standard deviation for DASUD, SID, GDE and AN considering likely and pathological initial load distributions for hypercubes attending to the initial distribution patterns and shapes

Torus (*standard deviation - σ*)									
	Shape	*likely distributions*				*pathological distributions*			
		25%	50%	75%	100%	25%	50%	75%	n-1
DASUD	SM	0.31	0.31	0.31	0.31	0.34	0.34	0.35	0.35
	Chain	0.3	0.31	0.31	0.31	0.35	0.34	0.33	
SID	SM	5.42	7.87	9.65	10.89	9.63	10.69	11.78	10.89
	Chain	2.37	3.12	3.62	4.24	7.23	6.95	5.19	
GDE	SM	0.8	0.8	0.84	0.85	0.87	0.86	0.87	0.88
	Chain	0.82	0.8	0.83	0.85	0.86	0.86	0.86	
AN	SM	0.14	0.14	0.14	0.14	0.18	0.18	0.18	0.17
	Chain	0.14	0.14	0.14	0.14	0.16	0.16	0.16	

Table B.8 Standard deviation for DASUD, SID, GDE and AN considering likely and pathological initial load distributions for torus attending to the initial distribution patterns and shapes

Hypercube (*load units – u's*)									
	Number of Proc.	*likely distributions*				*pathological distributions*			
		25%	50%	75%	100%	25%	50%	75%	n-1
DASUD	8	41.80	150.95	198.1	337.5	268	423	519	1128
	16	45.8	89.3	138.2	175.25	150	239.5	477.5	883
	32	35.4	61.35	93.3	124.75	79.5	110.5	268	718
	64	24.05	46.75	63.4	82.9	43.5	74	143.5	608
	128	15.65	32.35	47.6	59.95	31	46	91	536
SID	8	74.2	142.85	194	332.9	265.5	421	517	1125
	16	36.55	78.35	127.35	164.6	144	220	470	874
	32	23.1	48.35	80.4	111.85	60.5	95	257	706
	64	9.65	27.2	44.1	61.05	21	52.5	119	579
	128	3.55	12.85	22.45	31.9	7.5	16	59	485
GDE	8	79.8	189.7	234.7	441.3	540.2	723.1	834.7	1659
	16	70.2	120.7	170.3	221.7	275.1	381.2	509.1	1167
	32	452	84.2	112.7	122.5	198.1	268.7	395.4	1017
	64	10.8	28.5	56.7	67.2	230.1	471.8	562.1	1360
	128	19.5	33.2	49.3	67.4	72.1	101.7	173.1	908
AN	8	137.2	282.95	354.35	585.1	723	954.5	932.5	1860
	16	86	169.15	268.85	345.9	336.5	596.5	761.5	1474
	32	54.15	102.8	154.55	211.3	211	307	459	1177
	64	27.25	60.1	86.95	112.25	110.5	192.5	273.5	995
	128	18.9	31.2	49.2	66.1	68.5	97.5	161	801

Table B.9 Load units (u) for DASUD, SID, GDE and AN considering likely and pathological initial load distributions for hypercubes attending to the architecture size and initial distribution patterns.

Torus (*load units – u's*)									
	Number of Proc.	*likely distributions*				*pathological distributions*			
		25%	50%	75%	100%	25%	50%	75%	n-1
DASUD	9	69.9	141.7	193.85	251.1	181.5	212	365.5	836
	16	46.95	89.8	137.2	175.6	149	238	477	881
	36	33.35	73.15	108.6	137.15	115	172	329.5	1067
	64	21.5	46.05	67.9	94.2	87	130	231.5	1169
	121	15.95	28.7	41.05	54.95	61.5	93.5	158.5	1253
SID	9	33.85	137.8	189.65	246.5	179	208	360.5	832
	16	36.55	78.85	127.95	164.45	144	221	471	876
	36	21.9	59.9	92.75	123.35	88.5	156.5	306	1045
	64	7.75	23.15	42.65	66.25	42	92	197	1132
	121	3	6.8	11	17.85	15.5	36.5	115.5	1175
GDE	9	321.5	438.7	594.5	793.4	528.3	971.4	2130.6	4113.7
	16	271.7	370.2	460	656.8	489.1	824.7	1875.1	3867.3
	36	99.3	166.4	298.2	399.9	379.1	834.7	1578.3	2670.2
	64	98.6	165.3	206.5	269.9	287.6	687.9	1356.9	2447.6
	121	53.8	97.2	126.8	179.7	144.7	435.9	894.2	1689.3
AN	9	163.55	291.6	416.7	592.85	703	1104	1212	1434
	16	37.05	77.4	120.75	154.6	159	241	425.5	764
	36	24.9	58.65	88.2	115.65	119	164.5	245	841
	64	30.85	70.75	106.8	156.4	157	250.5	434.5	1770
	121	12.35	23	35.3	50.75	58.5	89.5	154.5	955

Table B.10 Load units (u) for DASUD. SID. GDE and AN considering likely and pathological initial load distributions for torus attending to the architecture size and initial distribution patterns

Hypercube (*load units- u's - by shapes)*									
	Shape	*likely distributions*				*pathological distributions*			
		25%	50%	75%	100%	25%	50%	75%	n-1
DASUD	SM	40.32	71.26	97.6	144.18	107.4	163	324.4	781.4
	Chain	36.92	80.24	118.74	167.1	126.6	197.4	279	
SID	SM	26.58	52.12	77.5	123.56	87.6	142.6	297.8	753.8
	Chain	32.24	71.72	109.82	157.38	111.8	179.2	271	
GDE	SM	51.1	99.8	93.8	197.3	280.3	428.9	584.9	1222.2
	Chain	39.1	82.7	71.2	170.5	245.9	349.7	304.7	
AN	SM	76.42	155.5	217.38	319.52	289.4	487.8	782.8	1261.4
	Chain	53.9	102.98	143.46	208.84	290.4	363.8	252.2	

Table B.11 Load units (u) for DASUD, SID, GDE and AN considering likely and pathological initial load distributions for hypercubes attending to the initial distribution patterns and shapes

Torus (*load units- u's - by shapes)*									
	Shape	*likely distributions*				*pathological distributions*			
		25%	50%	75%	100%	25%	50%	75%	n-1
DASUD	SM	36.27	74.76	105.42	137.42	121.6	175.4	343.6	1041.2
	Chain	38.8	77	114.04	142.12	116	162.8	281.2	
SID	SM	22.7	55.08	82.42	117.74	92.2	145.2	293.6	1012
	Chain	31.52	67.52	107.34	129.62	95.4	140.4	263.2	
GDE	SM	192.6	281.3	367.4	487.9	397	786.8	1789.1	2957.6
	Chain	145.3	213.7	307.1	431.9	334.6	714.9	1344.9	
AN	SM	58.76	115.02	121.22	179.52	253.8	375	540.8	1152.8
	Chain	48.72	82.29	137.52	196.76	224.8	365.4	447.8	

Table B.12 Load units (u) for DASUD, SID, GDE and AN considering likely and pathological initial load distributions for torus attending to the initial distribution patterns and shapes

Hypercube (*steps*)									
	Number	*likely distributions*				*pathological distributions*			
	of Proc.	25%	50%	75%	100%	25%	50%	75%	n-1
D	8	17.65	17.45	18.65	19.35	15.5	15.5	13	21
A	16	24.95	27.95	29	30.45	21.5	34.5	26	32
S	32	25.6	29.5	31.65	32.55	39.5	35	32	42
U	64	22.4	32.55	37.9	39.75	41.5	36	40.5	53
D	128	16.9	26.55	34.65	40.2	31.5	38.5	45	61
	8	8.15	8.3	8.75	9.65	9	8.5	7	11
S	16	7.55	9.75	11	11.45	8	14	11	13
I	32	6.45	8.7	10.55	10.75	12.5	10.5	11.5	15
D	64	3	7.55	9.3	9.75	8	10.5	10	12
	128	1.6	3.25	5.55	7.35	3.5	6	8	9
	8	17.78	18.43	19.02	19.78	20.5	22.35	23	24.5
G	16	26.48	26.67	27.95	28.85	30	35	37.5	38.5
D	32	36.9	37.8	38.25	39.11	53.5	56	59.5	61.5
E	64	46.23	46.86	47.97	48.78	57.5	59	60.5	63
	128	43.2	43.9	46.34	46.11	61	62.5	65.5	70
	8	29	31.2	31	34.8	28	36	44	40
A	16	31.8	35	37.8	39.8	40	36	42	56
N	32	31	36	37.6	40.2	40	44	38	48
	64	29.2	34.2	37	41	42	44	38	60
	128	26.8	31.6	34.6	37.4	44	38	48	54

Table B.13 Simulations steps (steps) for DASUD, SID, GDE and AN considering likely and pathological initial load distributions for hypercubes attending to the architecture size and initial distribution patterns.

Torus (*steps*)									
	Number of Proc.	*likely distributions*				*pathological distributions*			
		25%	50%	75%	100%	25%	50%	75%	n-1
DASUD	9	13.55	17.3	18.15	18.7	18	18	20.5	22
	16	25.25	27.95	28.6	30.4	20	32	26	33
	36	24.6	33.75	37.9	41.25	51	47.5	49.5	66
	64	20.85	35.55	43.95	53.75	54	69	63	96
	121	18.55	28.45	36.65	46.7	51	73	83.5	125
SID	9	6.8	8.55	8.7	9.15	9	9	8.5	12
	16	7.55	10.05	11.5	11.45	8	14	11.5	14
	36	7.8	15.25	17.5	20.5	22	24	22	31
	64	2.55	9.15	15.4	22.7	12.5	31	29.5	62
	121	1.55	2.45	3.15	6.75	6.5	17.5	40.5	74
GDE	9	49.7	50.2	51.4	52.7	60.5	61.5	62	61
	16	48.45	49.7	51.62	53.21	61.5	62.5	65	66
	36	45.7	46.91	48.4	52.41	63.5	65.5	67	69
	64	46.5	48.73	50.67	52.5	68.5	71	72.5	73
	121	48.46	50.67	52,42	53.9	76.5	79.5	81	83
AN	9	49.6	51.6	55.2	57.2	60	72	60	64
	16	7.65	8.6	9.55	9.75	10	10	10	11
	36	8.7	10.75	11.5	11.65	12	14.5	13	16
	64	35.8	45	49.6	55.8	60	62	64	92
	121	10.4	13	15.05	17	18.5	21	22.5	29

Table B.14 Simulations steps (steps) for DASUD. SID. GDE and AN considering likely and pathological initial load distributions for torus attending to the architecture size and initial distribution pattems

Hypercube (*steps - by shapes)*									
	Shape	*likely distributions*				*pathological distributions*			
		25%	50%	75%	100%	25%	50%	75%	n-1
DASUD	SM	12.5	17.26	19.62	21.8	17.4	20.8	24	24.2
	Chain	6.62	9.68	10.9	11.76	14	13.6	10	[redacted]
SID	SM	6.04	8.48	10.52	11.84	9.8	12	12.4	12
	Chain	4.66	6.54	7.54	7.74	6.6	7.8	6.6	[redacted]
GDE	SM	37.93	38.37	39.35	46.92	48.85	51.38	41.06	51.5
	Chain	30.27	31.1	32.47	43.28	40.17	42.64	35.86	[redacted]
AN	SM	30.8	35.28	38.24	41.92	39.2	41.6	47.2	51.2
	Chain	28.32	31.92	32.96	35.36	38.4	37.6	28.8	[redacted]

Table B.15 Steps for DASUD, SID, GDE and AN considering likely and pathological initial load distributions for hypercubes attending to the initial distribution patterns and shapes

Torus (*steps - by shapes)*									
	Shape	*likely distributions*				*pathological distributions*			
		25%	50%	75%	100%	25%	50%	75%	n-1
DASUD	SM	26.22	37.32	43.86	51	43	56	65.2	68
	Chain	18.78	19.68	22.18	25.32	34.6	39.6	31.2	[redacted]
SID	SM	6.24	11.88	15.58	19.68	12.8	23.6	35	38.6
	Chain	4.26	6.3	6.92	8.54	10.4	14.6	9.8	[redacted]
GDE	SM	51.21	51.76	53.05	54.85	67.85	69.31	70.73	70.4
	Chain	44.25	46.78	48.79	51.09	64.38	66.3	68.3	[redacted]
AN	SM	23.9	27.32	30.48	32.5	34	35.8	37.2	42.4
	Chain	20.96	24.2	25.88	28.06	30.2	36	30.6	[redacted]

Table B.16 Load units (u) for DASUD, SID, GDE and AN considering likely and pathological initial load distributions for torus attending to the initial distribution patterns and shap

Appendix C

Scalability of DASUD: *complementary figures*

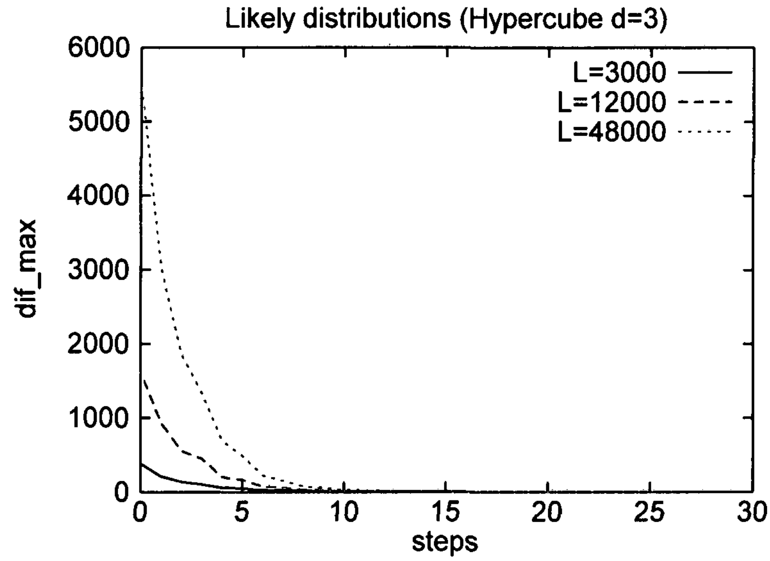

(a)

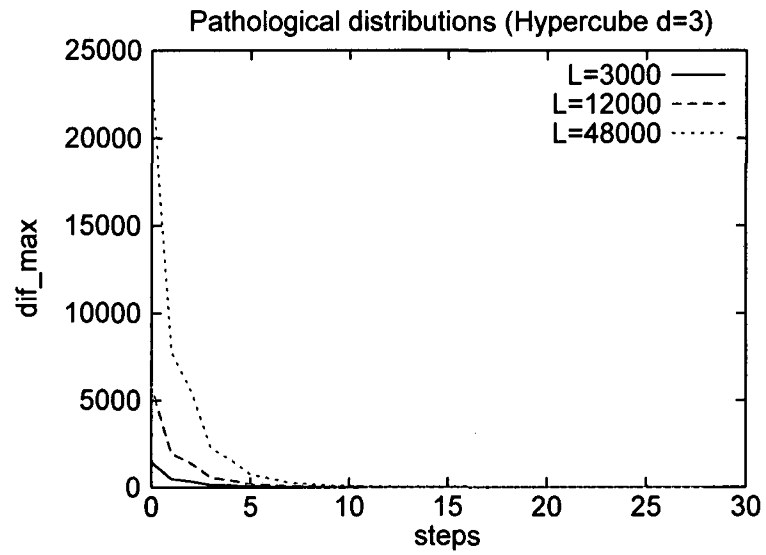

(b)

Figure C.1 Influence of the problem size in the global dif_max as the load-balancing process goes on for a 3-dimensional hypercube for likely (a) and pathological (b) initial load distributions.

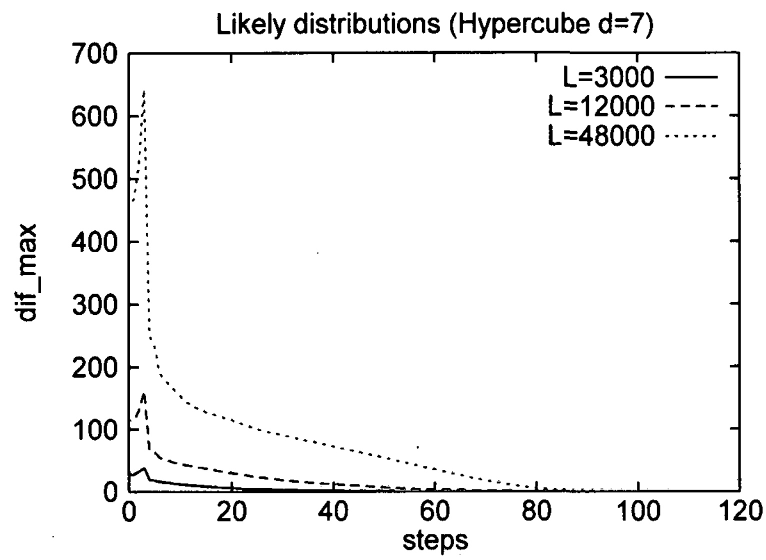

(a)

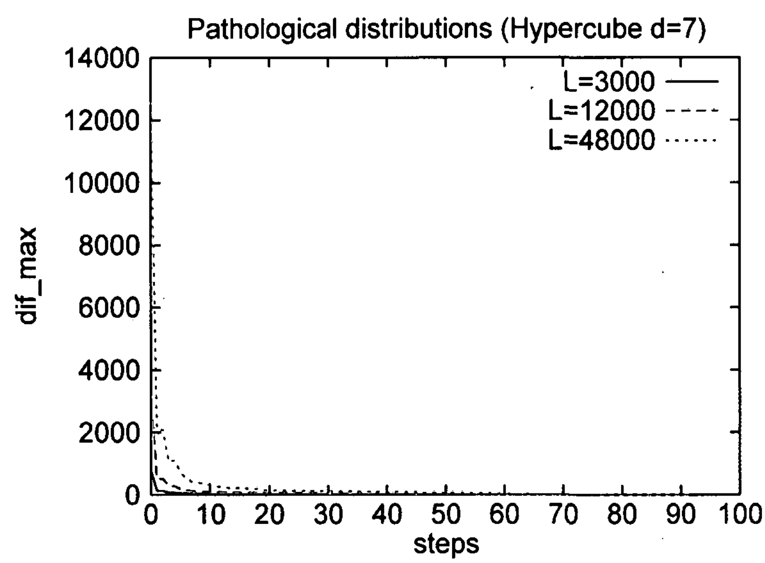

(b)

Figure C.2 Influence of the problem size in the global dif_max as the load-balancing process goes on for a 7-dimensional hypercube for (a) likley and pathological (b) initial load distributions.

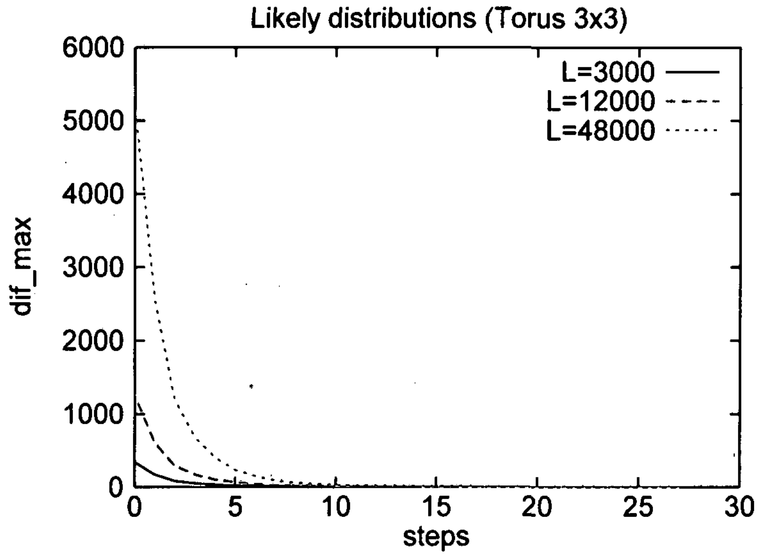

(a)

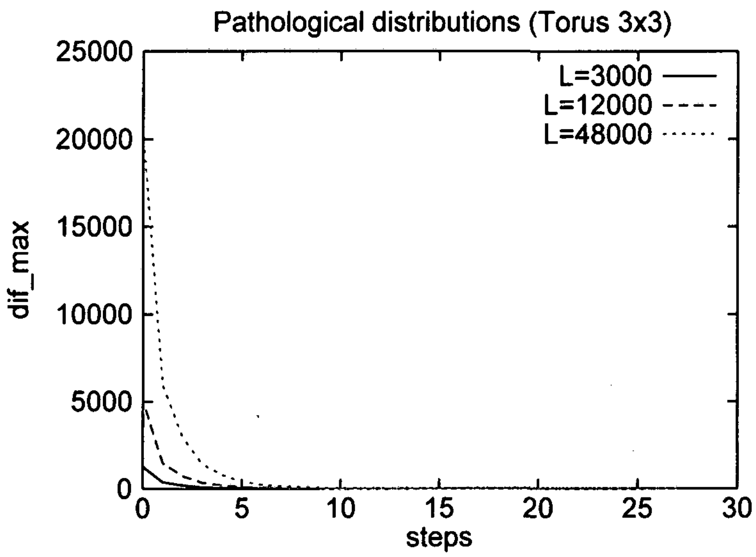

(b)

Figure C.3 Influence of the problem size in the global dif_max as the load-balancing process goes on for a 3x3 torus for likely (a) and pathological (b) initial load distributions.

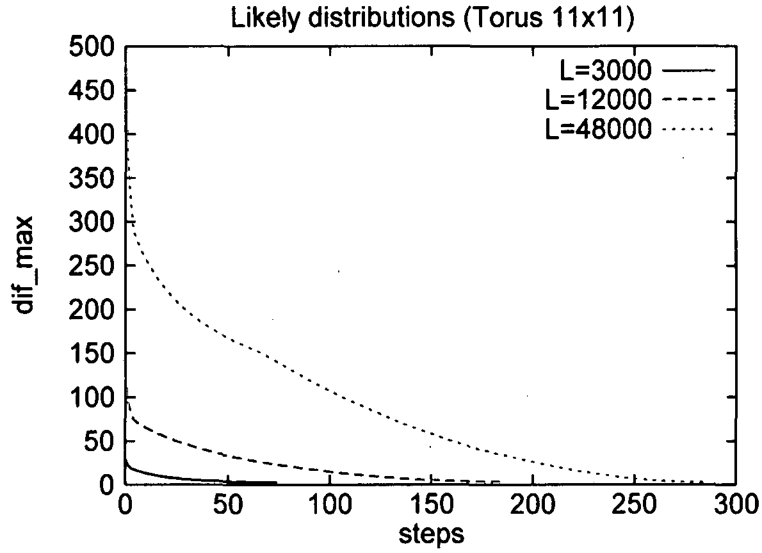

(a)

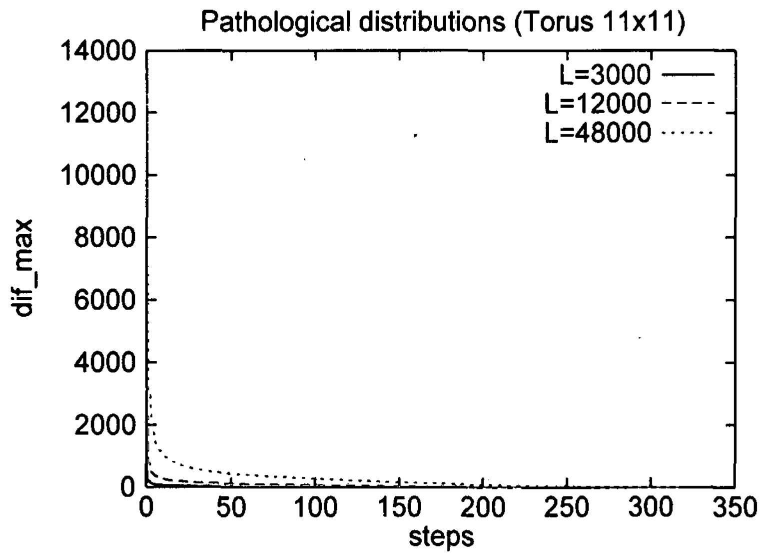

(b)

Figure C.4 Influence of the problem size in the global dif_max as the load-balancing process goes on for a 11x1 torus for likely (a) and pathological (b) initial load distributions.

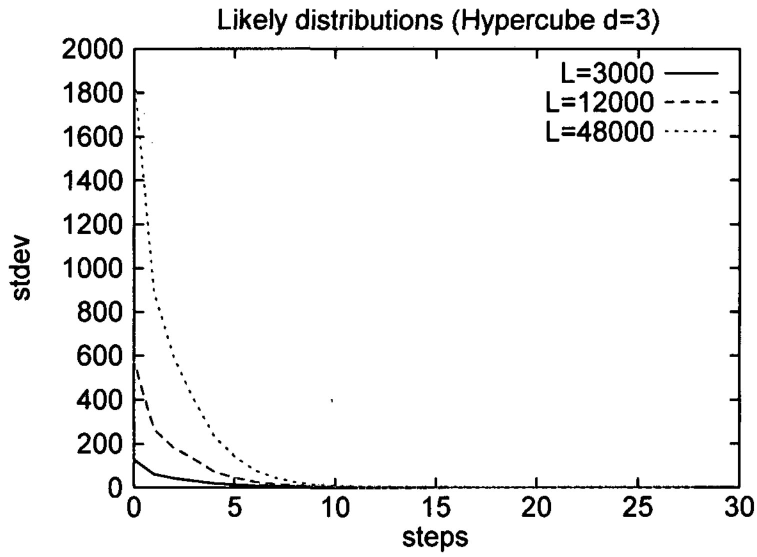

(a)

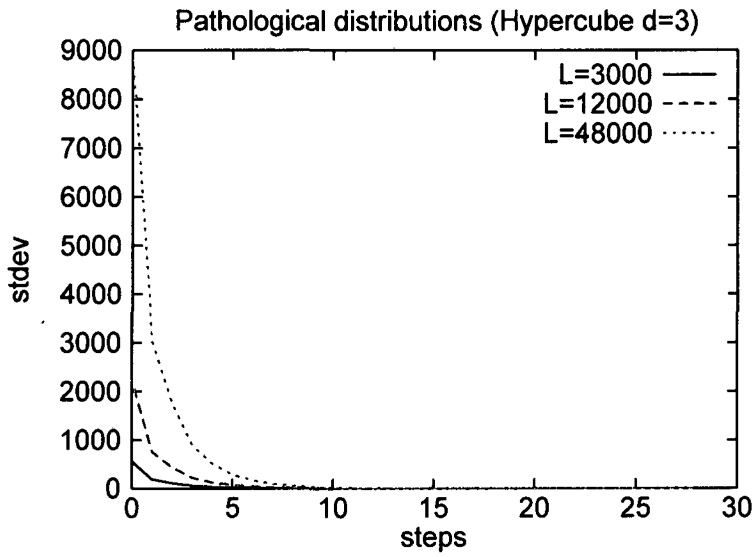

(b)

Figure C.5 Influence of the problem size in the global standard deviation as the load-balancing process goes on for a 3-dimensional hypercube for likely (a) and pathological (b) initial load distributions.

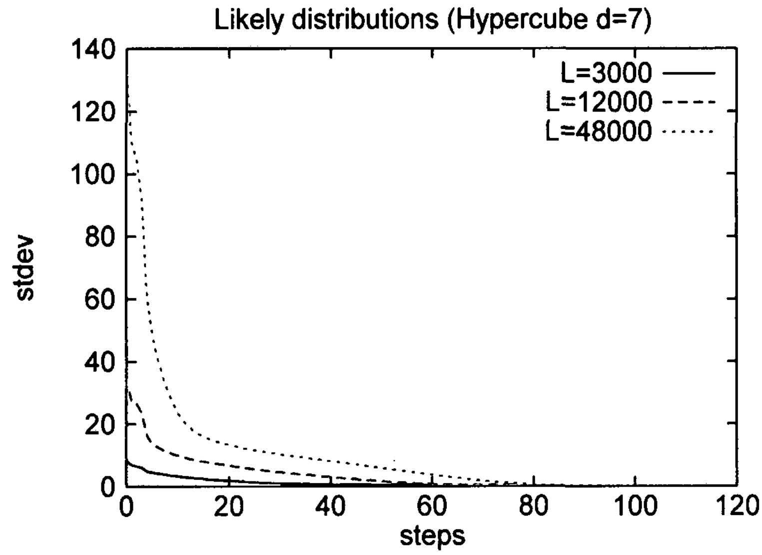

(a)

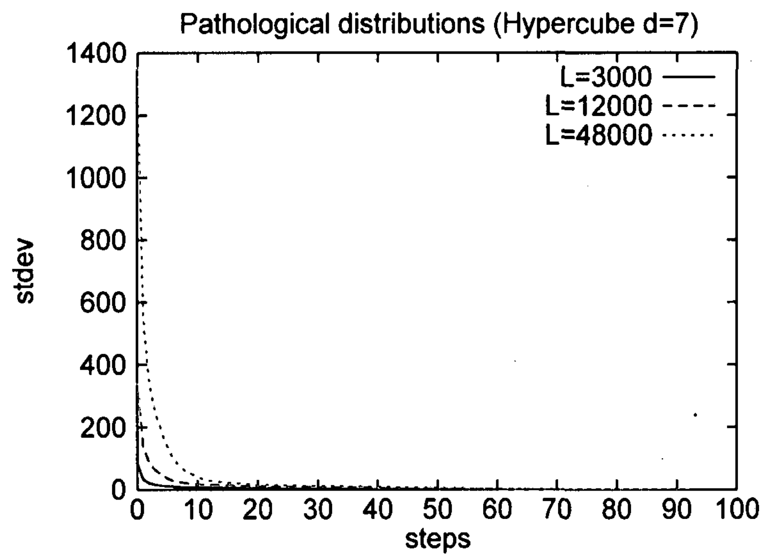

(b)

Figure C.6 Influence of the problem size in the global standard deviation as the load-balancing process goes on for a 7-dimensional hypercube for likely (a) and pathological (b) initial load distributions.

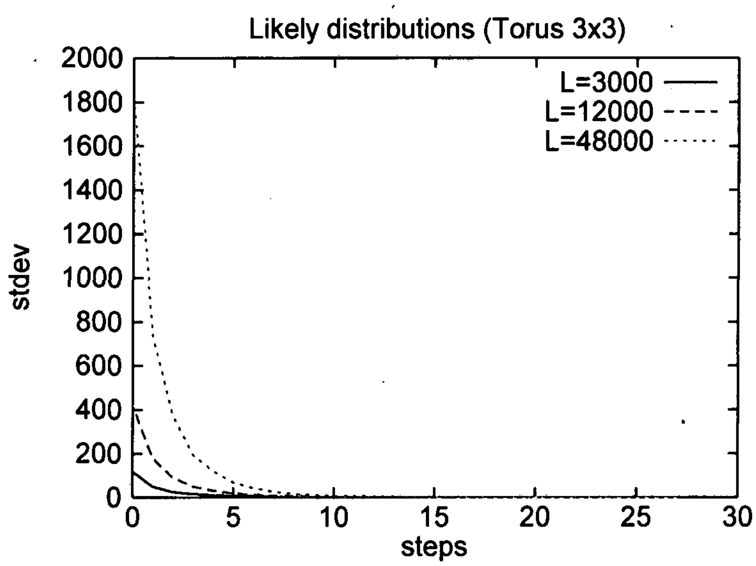

(a)

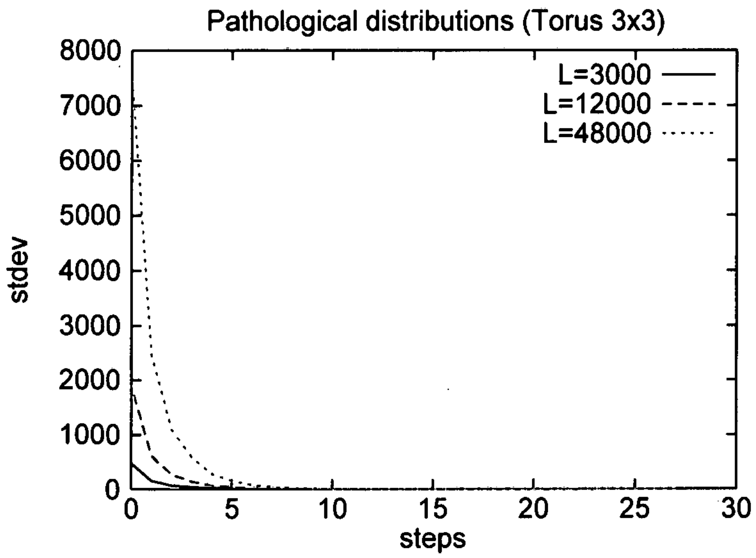

(b)

Figure C.7 Influence of the problem size in the global standard deviation as the load-balancing process goes on for a 3x3 torus for likely (a) and pathological (b) initial load distributions.

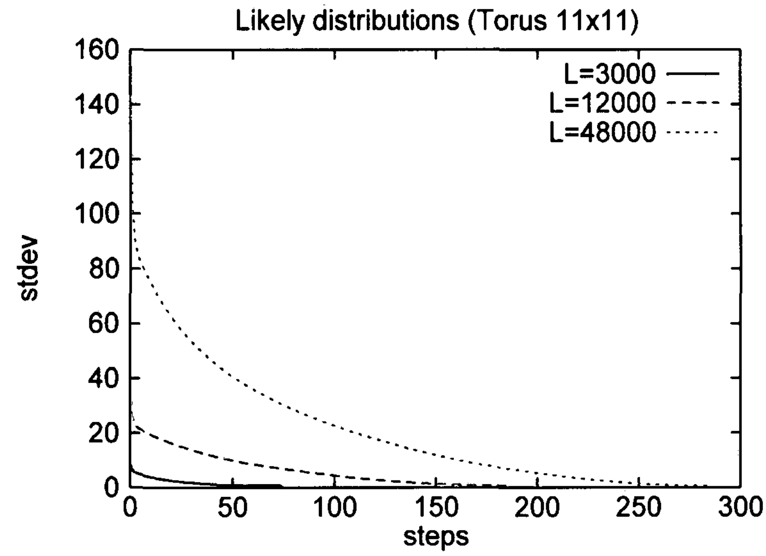

(a)

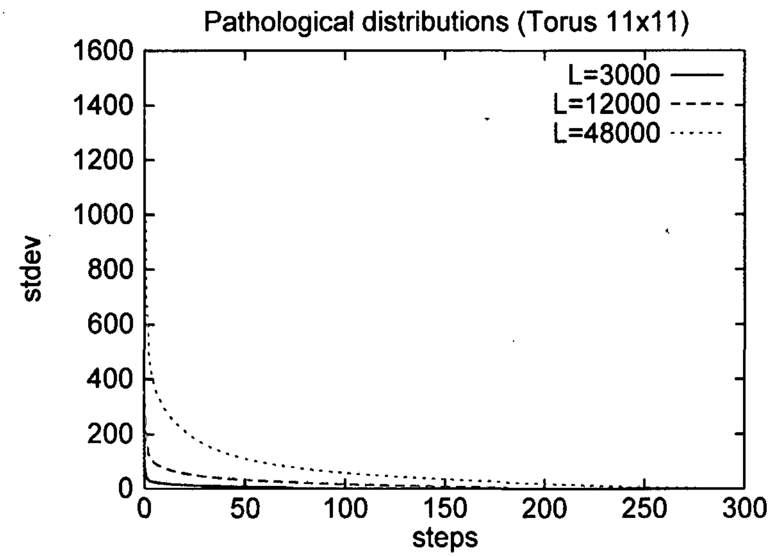

(b)

Figure C.8 Influence of the problem size in the global standard deviation as the load-balancing process goes on for a 11x11 torus for pathological initial load distributions.

Appendix D

Enlarging the domain (d_s-DASUD):

complementary figures and tables

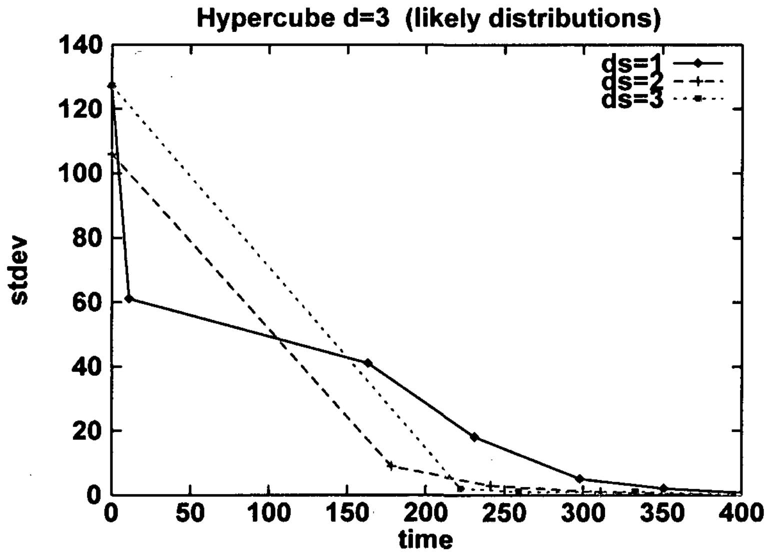

Figure D.1 Global load standard deviation versus time for a 3-dimensional hypercube varying ds from 1 to 3 for likely initial load distributions.

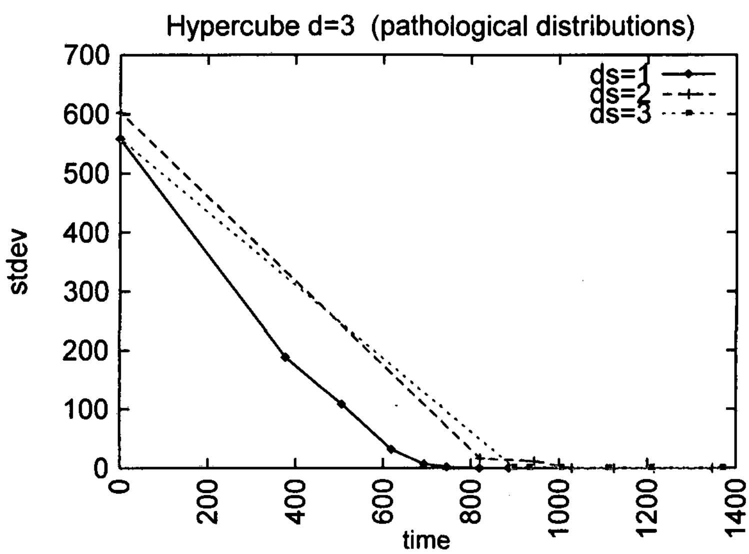

Figure D.2 Global load standard deviation versus time for a 3-dimensional hypercube varying ds from 1 to 3 for pathological initial load distributions.

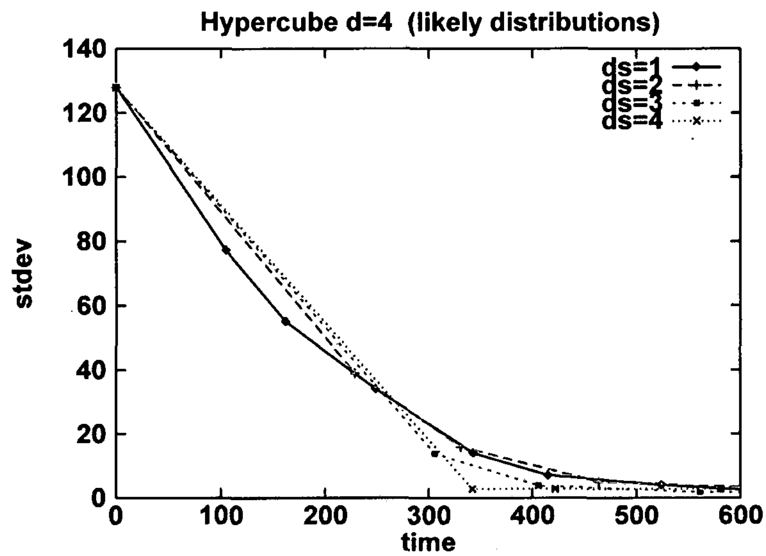

Figure D.4 Global load standard deviation versus time for a 4-dimensional hypercube varying ds from 1 to 4 for likely initial load distributions.

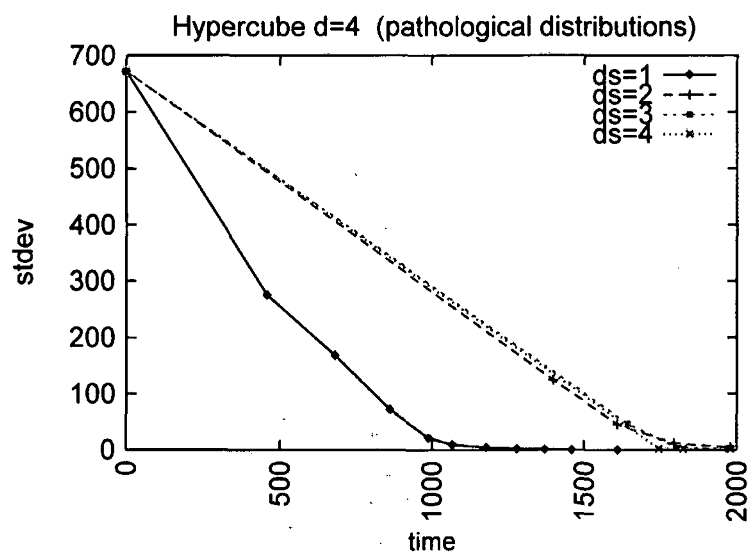

Figure D.5 Global load standard deviation versus time for a 4-dimensional hypercube varying ds from 1 to 4 for pathological initial load distributions.

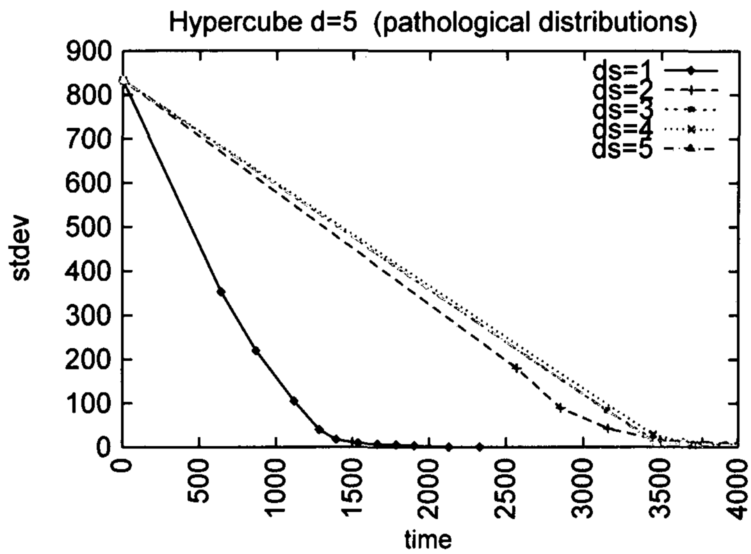

Figure D.6 Global load standard deviation versus time for a 5-dimensional hypercube varying ds from 1 to 5 for pathological initial load distributions.

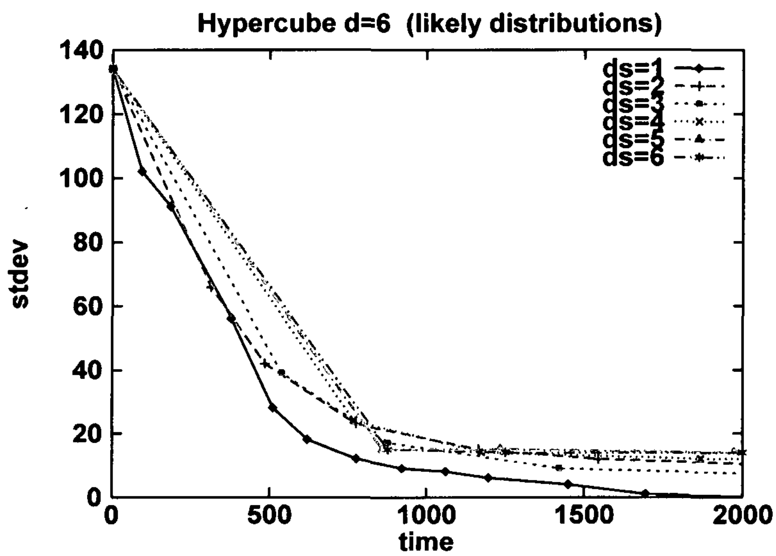

Figure D.7 Global load standard deviation versus time for a 6-dimensional hypercube varying ds from 1 to 6 for likely initial load distributions.

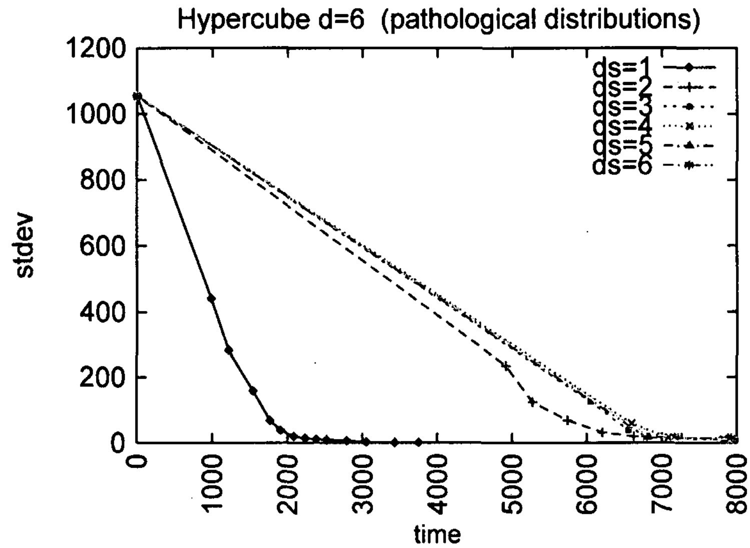

Figure D.8 Global load standard deviation versus time for a 6-dimensional hypercube varying ds from 1 to 6 for pathological initial load distributions.

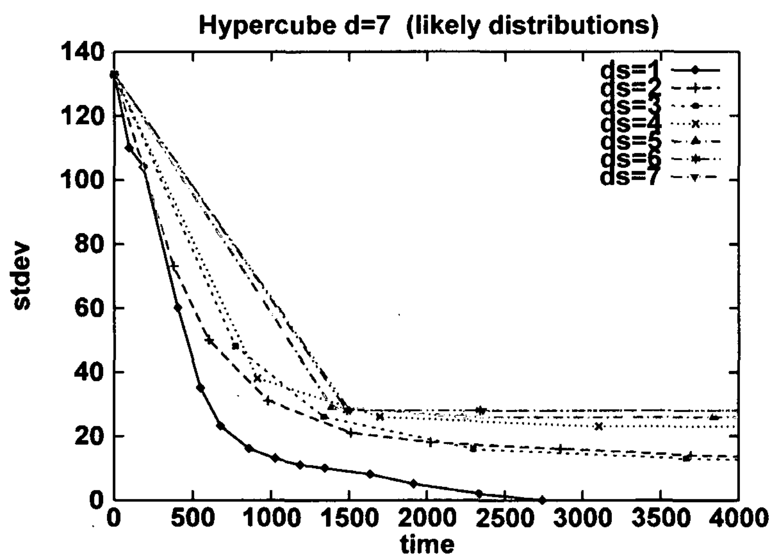

Figure D.9 Global load standard deviation versus time for a 7-dimensional hypercube varying ds from 1 to 7 for likely initial load distributions.

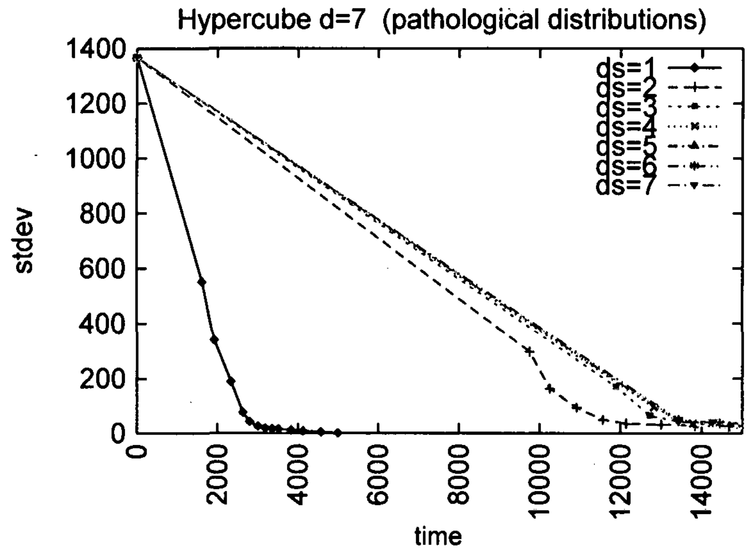

Figure D.10 Global load standard deviation versus time for a 7-dimensional hypercube varying ds from 1 to 7 for pathological initial load distributions.

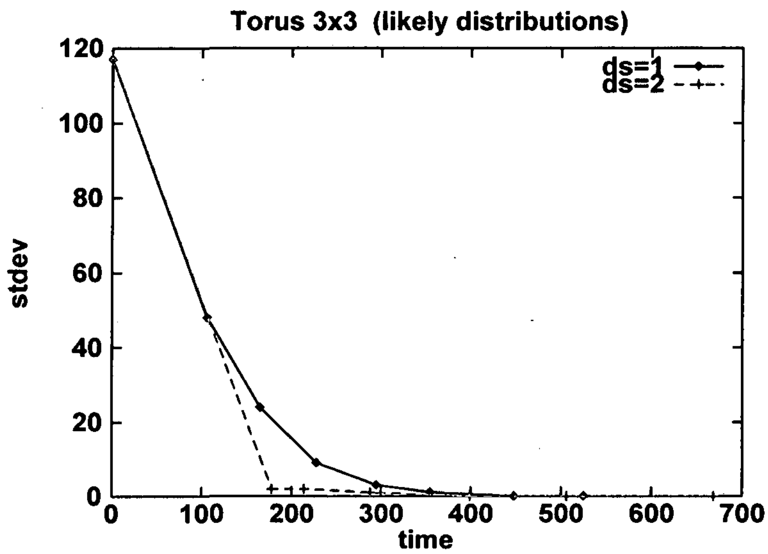

Figure D.11 Global load standard deviation versus time for a 3x3 torus varying ds from 1 to 2 for likely initial load distributions.

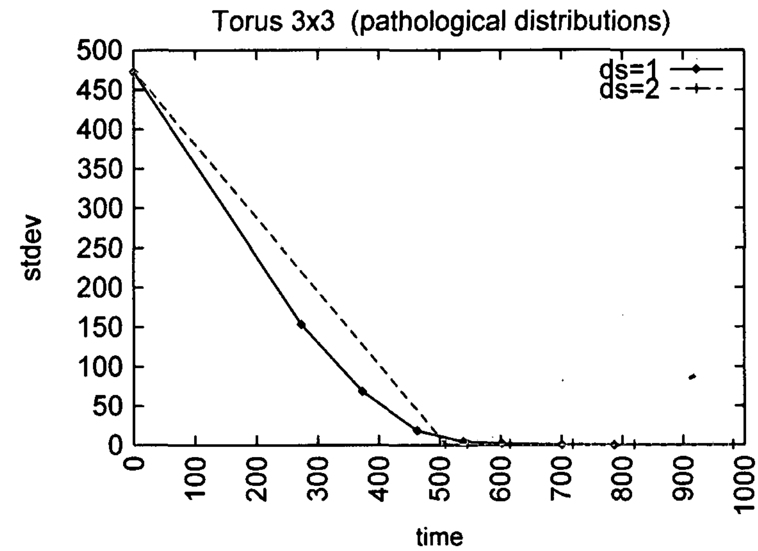

Figure D.12 Global load standard deviation versus time for a 3x3 torus varying ds from 1 to 2 for pathological initial load distributions.

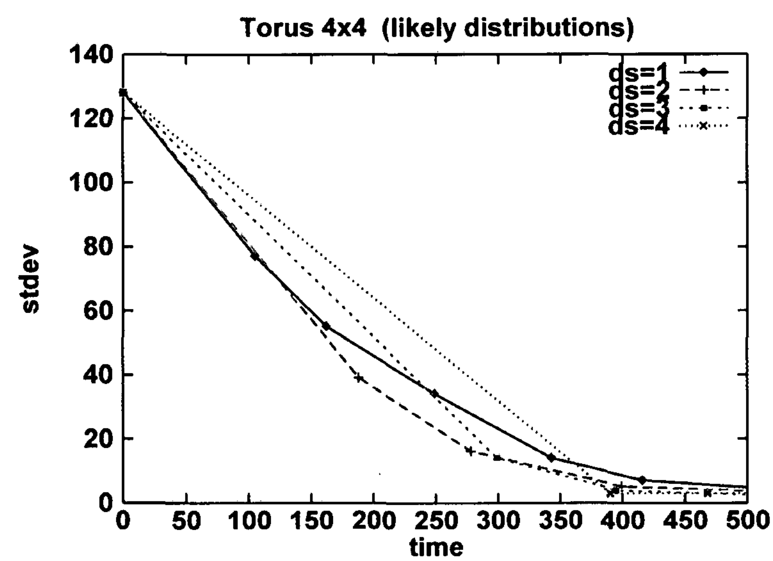

Figure D.13 Global load standard deviation versus time for a 4x4 torus varying ds from 1 to 4 for likely initial load distributions.

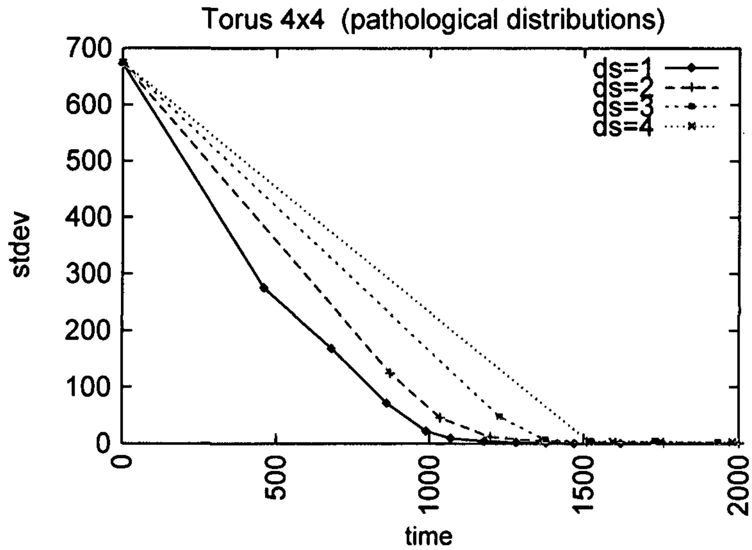

Figure D.14 Global load standard deviation versus time for a 4x4 torus varying ds from 1 to 4 for pathological initial load distributions.

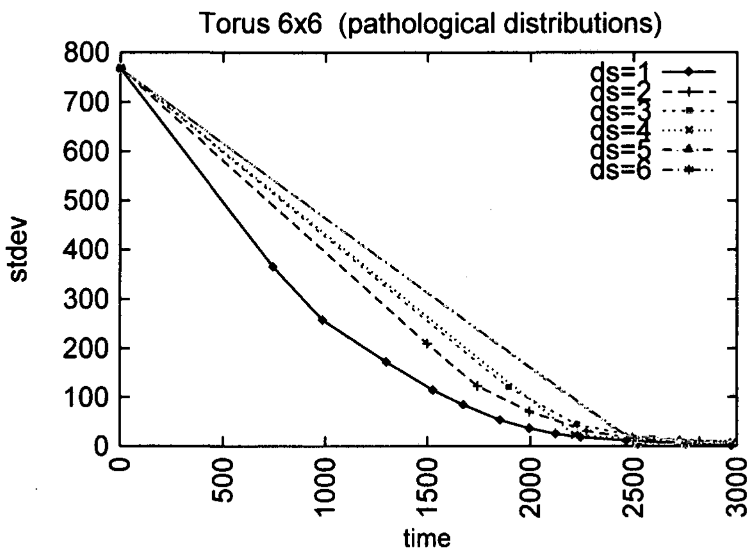

Figure D.15 Global load standard deviation versus time for a 6x6 torus varying ds from 1 to 6 for pathological initial load distributions.

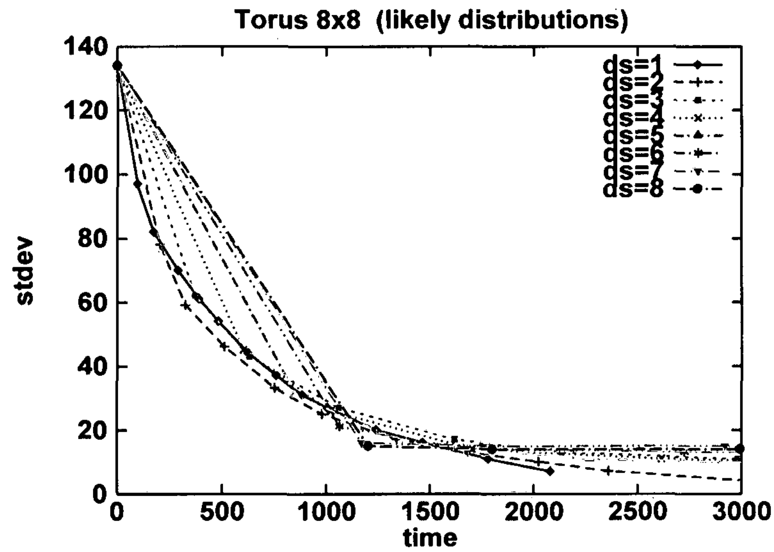

Figure D.16 Global load standard deviation versus time for a 8x8 torus varying ds from 1 to 8 for likely initial load distributions.

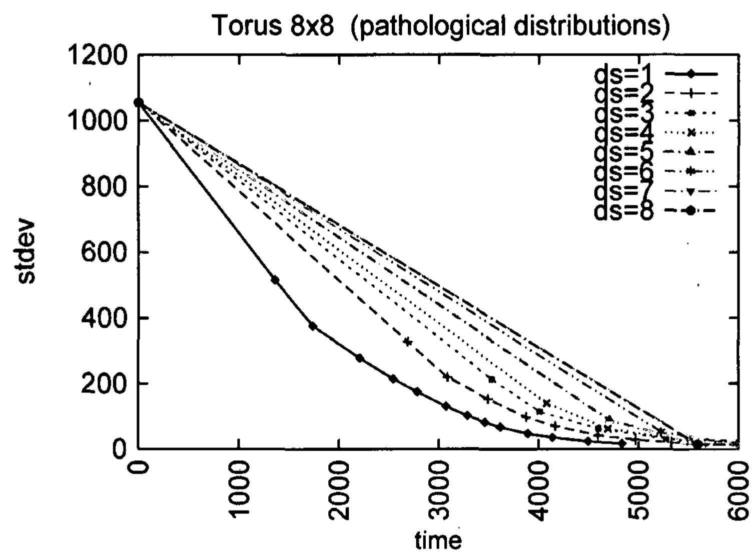

Figure D.17 Global load standard deviation versus time for a 8x8 torus varying ds from 1 to 8 for pathological initial load distributions.

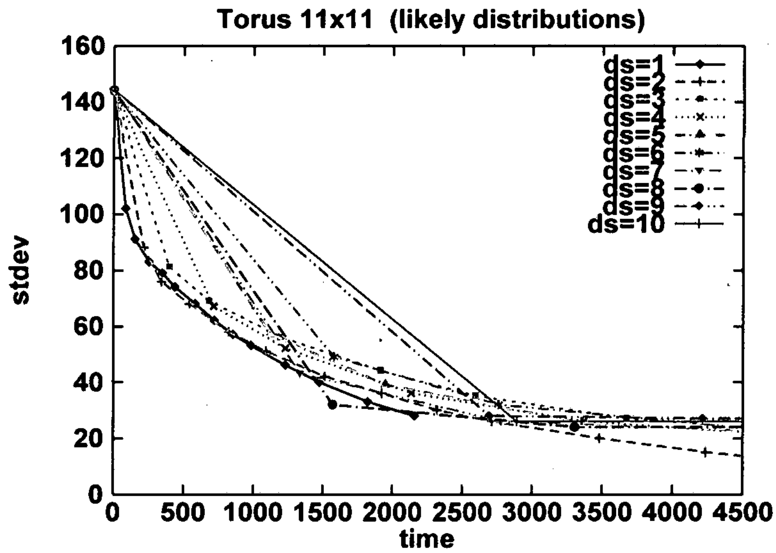

Figure D.18 Global load standard deviation versus time for a 11x11 torus varying ds from 1 to 10 for likely initial load distributions.

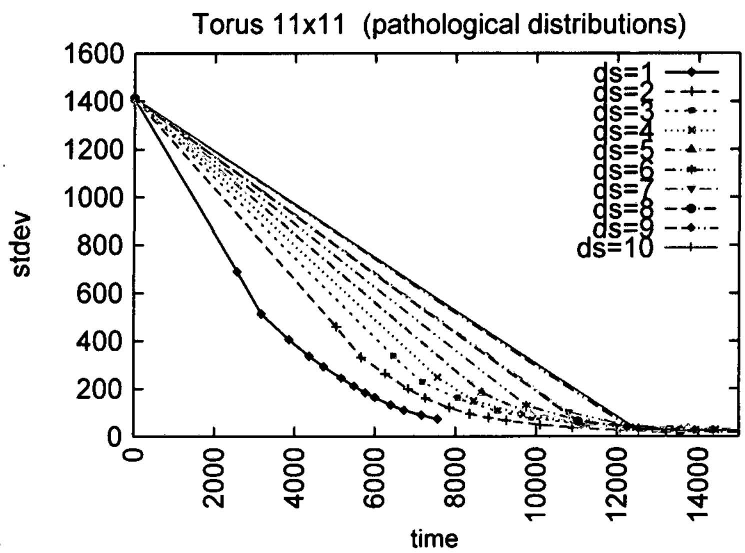

Figure D.19 Global load standard deviation versus time for a 11x11 torus varying ds from 1 to 10 for pathological initial load distributions.

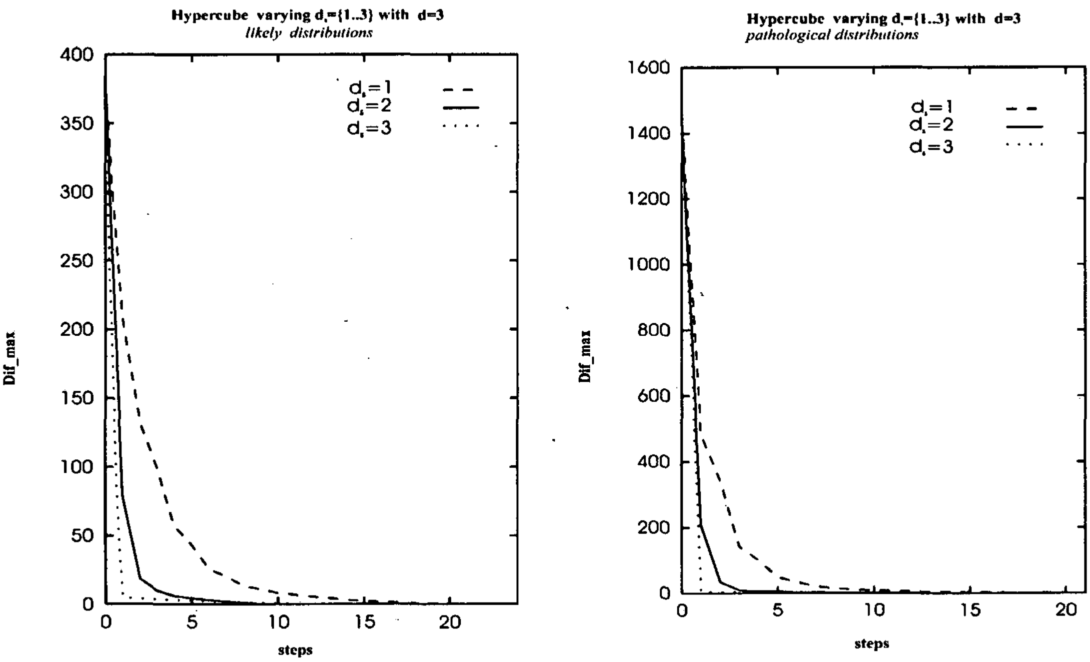

(a) (b)

Figure D.20 Global maximum load difference versus load-balancing steps for a 3-dimensional hypercube for likely (a) and pathological (b) initial load distribution for all possible domain scopes.

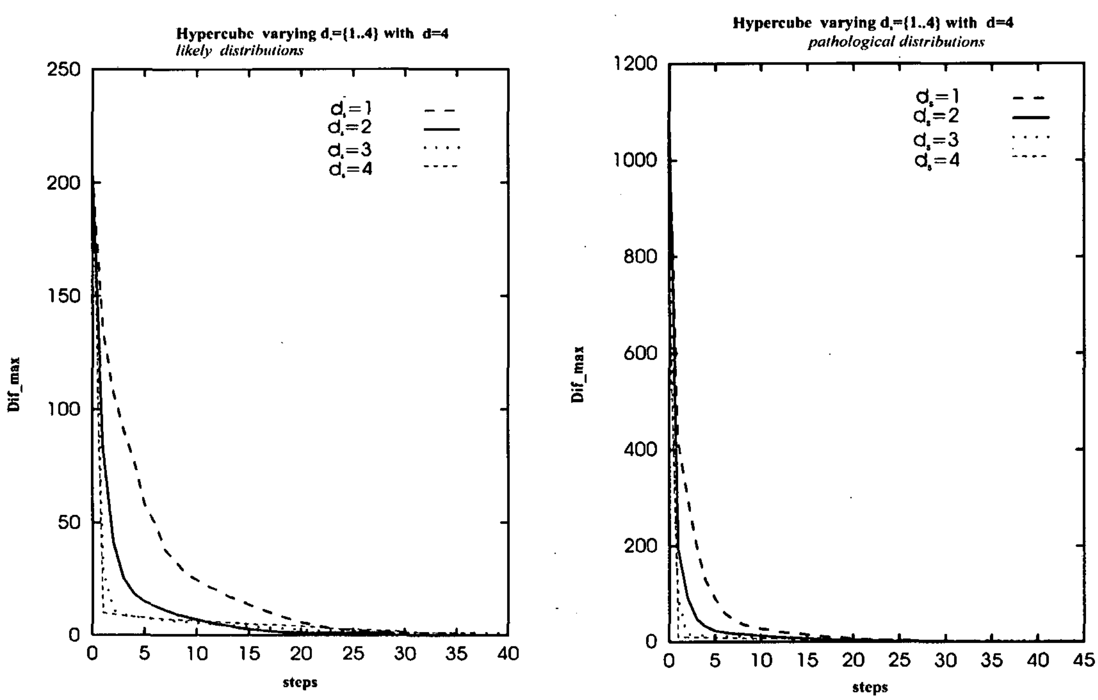

(a) (b)

Figure D.21 Global maximum load difference versus load-balancing steps for a 4-dimensional hypercube for likely (a) and pathological (b) initial load distribution for all possible domain scopes.

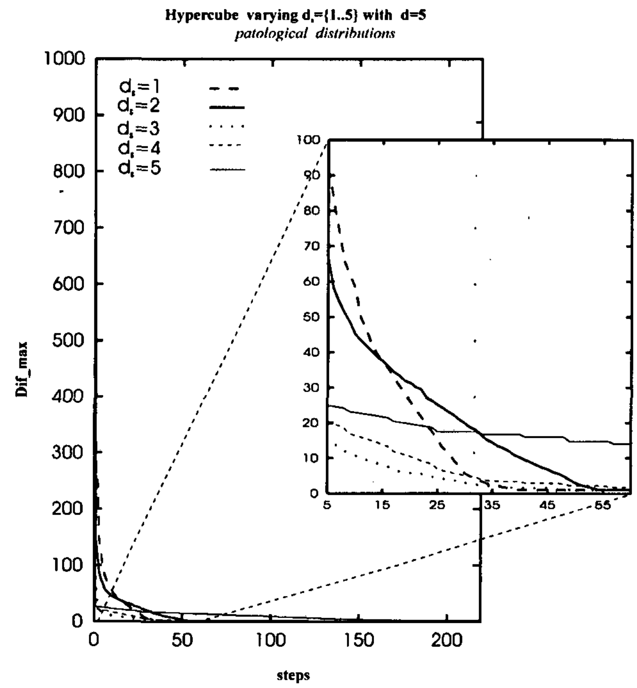

Figure D.22 Global maximum load difference versus load-balancing steps for a 5-dimensional hypercube for likely pathological initial load distribution for all possible domain scopes.

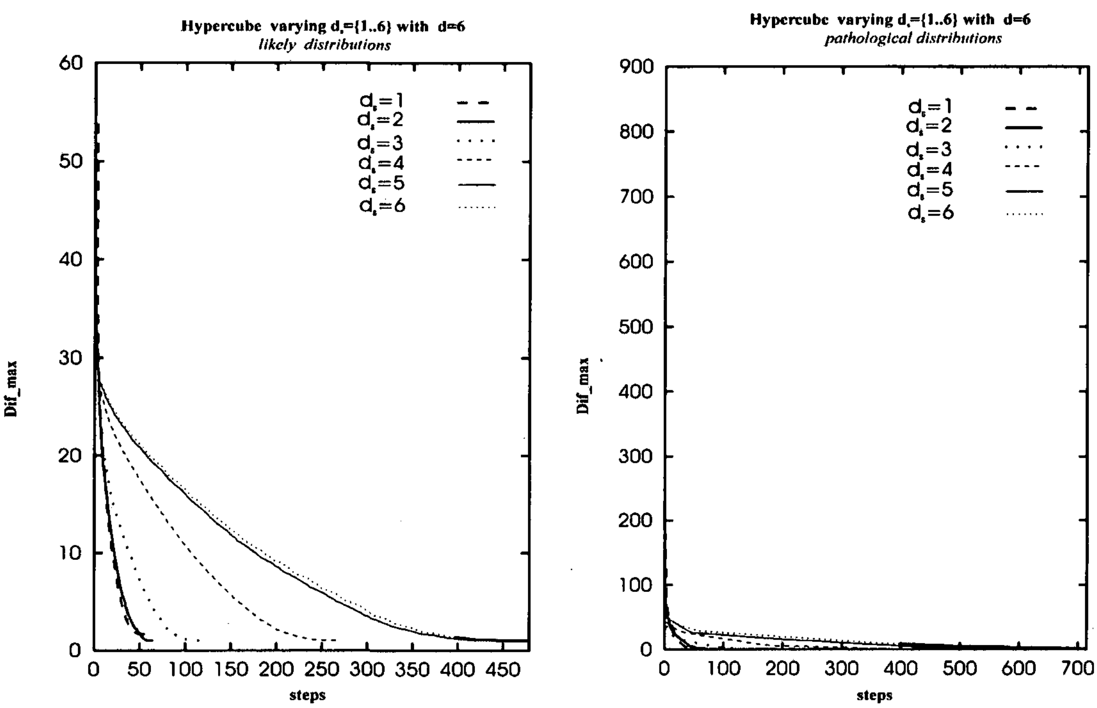

(a) *(b)*

Figure D.23 Global maximum load difference versus load-balancing steps for a 6-dimensional hypercube for likely (a) and pathological (b) initial load distribution for all possible domain scopes.

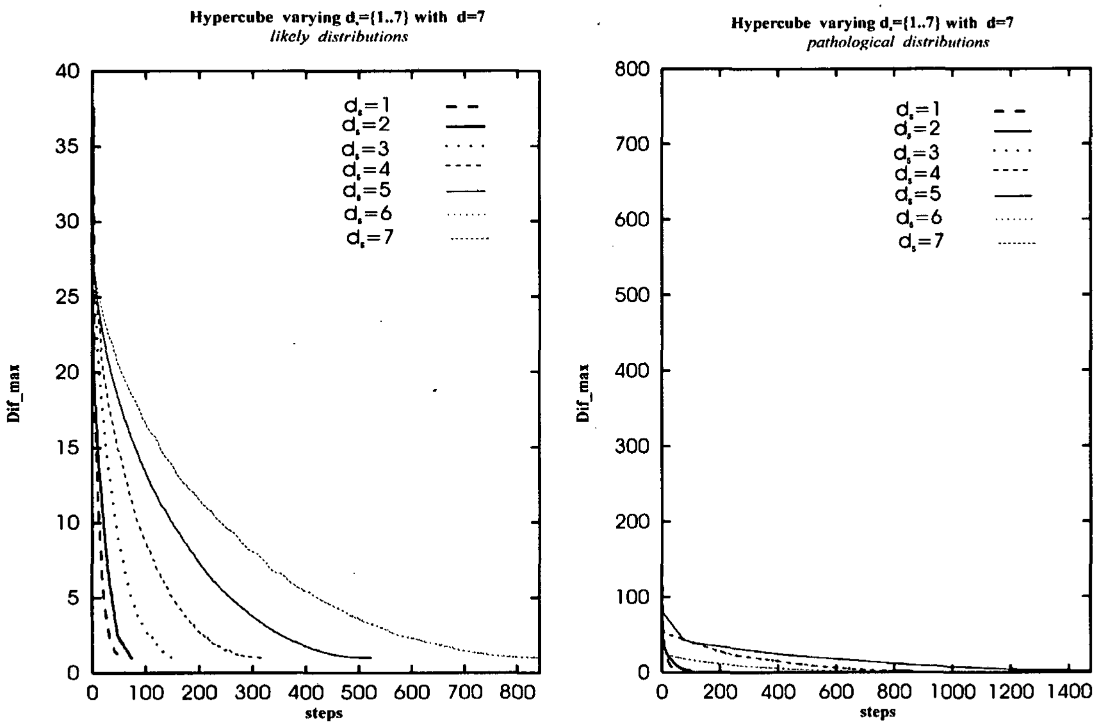

(a) (b)

Figure D.24 Global maximum load difference versus load-balancing steps for a 7-dimensional hypercube for likely (a) and pathological (b) initial load distribution for all possible domain scopes.

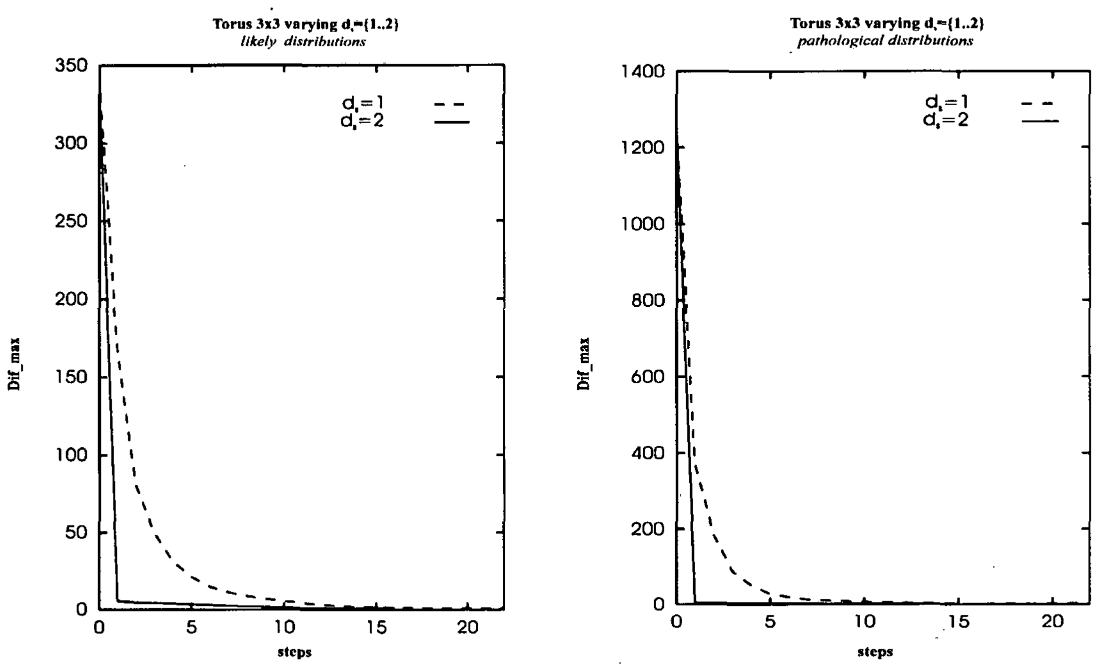

(a) (b)

Figure D.25 Global maximum load difference versus load-balancing steps for a 3x3 torus for likely (a) and pathological (b) initial load distribution for all possible domain scopes.

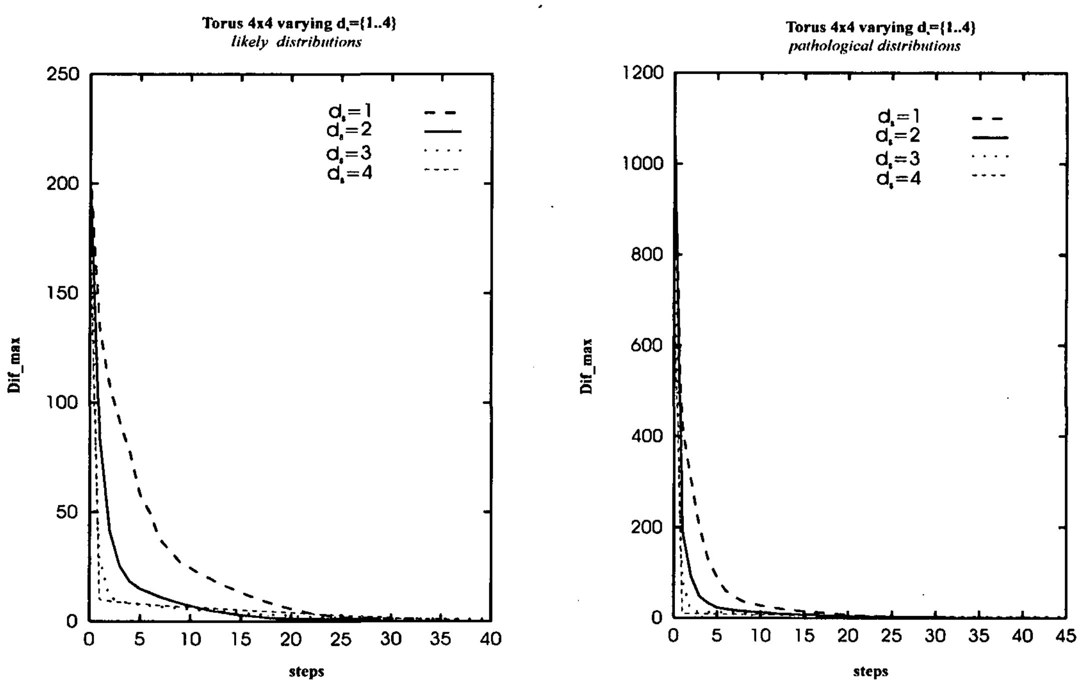

(a) (b)

Figure D.26 Global maximum load difference versus load-balancing steps for a 4x4 torus for likely (a) and pathological (b) initial load distribution for all possible domain scopes.

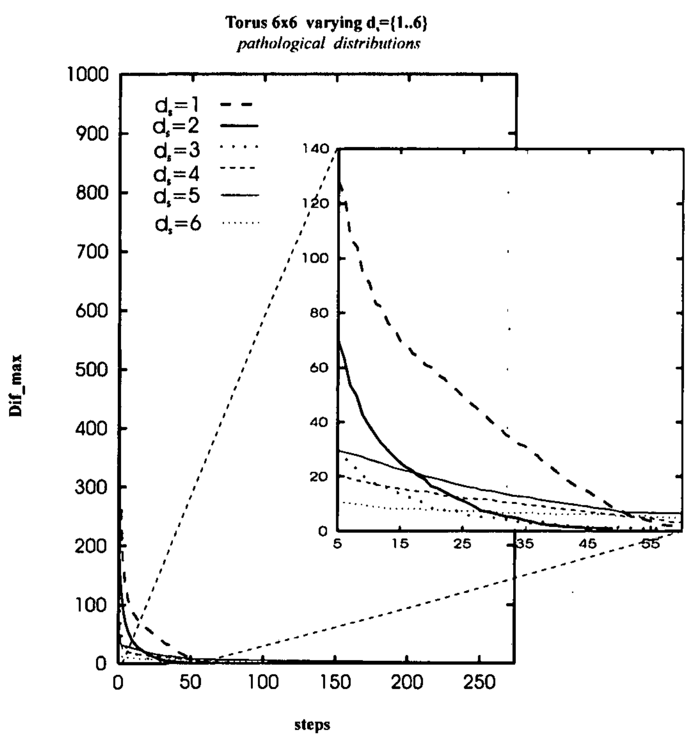

Figure D.27 Global maximum load difference versus load-balancing steps for a 6x6 torus for pathological initial load distribution for all possible domain scopes.

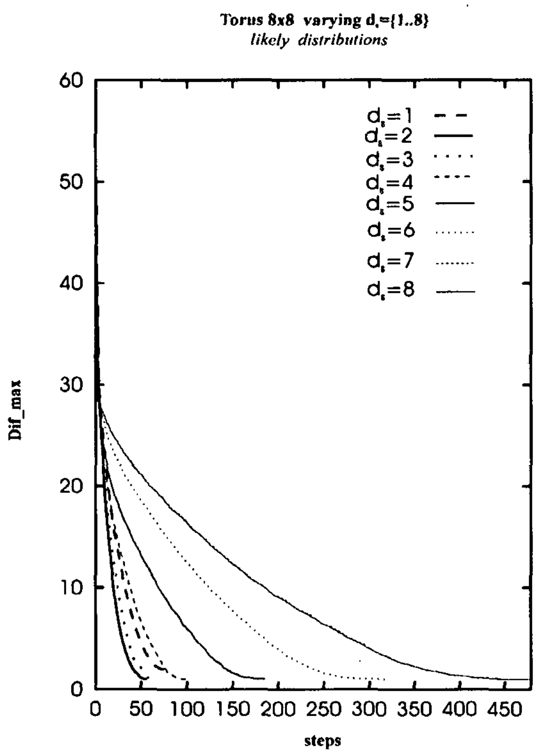

(a)

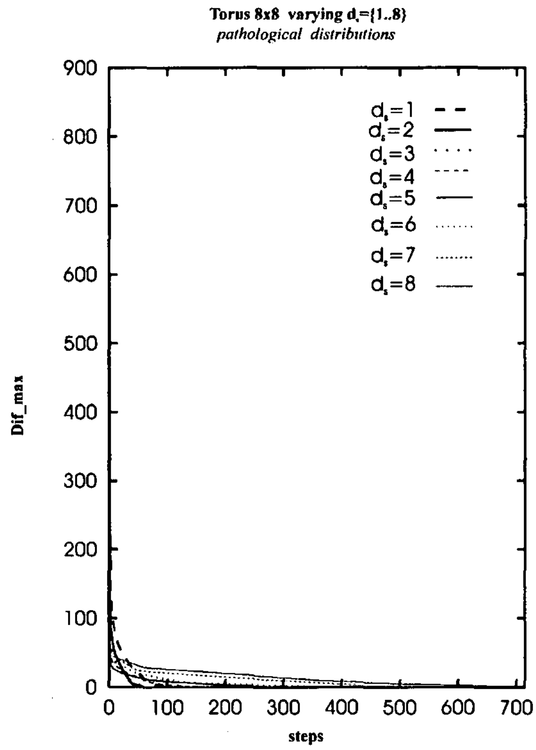

(b)

Figure D.28 Global maximum load difference versus load-balancing steps for a 8x8 torus for likely (a) and pathological (b) initial load distribution for all possible domain scopes.

Hypercube		*Pathological distributions*						
step		*0*	*4*			*7*		
d	d_s	*stdev*	*stdev*	*%*	*t_off*	*stdev*	*%*	*t_off*
3	1	558,30	31,82	94.3	19711,69	6,92	98.7	4806,29
	2	603,99	0,98	99.8	1009,13	0,35	99.9	393,59
	3	558,30	1,07	99.8	1075,80	0,40	99.9	444,81
4	1	673,35	71,16	89,43	61328,18	21,83	96.75	21607,44
	2	673,35	12,02	98,2	21585,52	5,29	99.2	10476,32
	3	673,35	3,71	99.44	7304,62	3,17	99.5	6950,46
	4	673,35	3,20	99.5	6334,13	2,91	99.5	6438,94
5	1	832,23	104,82	87.4	117309,30	39,96	95.1	51336,61
	2	832,23	42,15	94.9	133227,72	15,87	98.1	55470,01
	3	832,23	6,92	99.16	26240,12	5,87	99.2	24723,12
	4	832,23	6,21	99.25	25025,83	5,44	99.3	24714,06
	5	832,23	6,80	99.18	27282,62	6,64	99.2	30067,25
6	1	1054,37	157,18	85.09	242681,99	67,72	93.57	119867,79
	2	1054,37	68,05	93.5	390768,62	31,05	97.05	192731,23
	3	1054,37	13,16	98.75	94681,99	8,52	99.1	67979,50
	4	1054,37	11,15	98.9	87244,57	10,91	98.9	96445,76
	5	1054,37	11,77	98.8	94333,90	11,57	98.9	105509,14
	6	1054,37	14,33	98.6	113508,29	14,26	98.64	128854,43
7	1	1366,76	188,58	86.29	440453,11	75,78	94.4	199579,13
	2	1366,76	92,47	93.23	1009296,2	48,01	96.4	555034,01
	3	1366,76	28,20	97.9	390630,63	15,73	98.8	240758,66
	4	1366,76	23,96	98.2	366006,73	23,20	98.3	401729,34
	5	1366,76	15,93	98.8	255869,65	15,75	98.8	290876,91
	6	1366,76	35,08	97.43	566494,64	34,96	97.4	654147,92
	7	1366,76	36,23	97.3	582411,02	36,19	97.3	674370,43

Table D.1 Standard deviation, unbalance reduction percentage and trade-off between balance degree and time for hypercube topologies and for all possible d_s at different load-balancing steps for pathological initial load distributions

Torus		*Pathological distributions*						
step		*0*	*4*			*7*		
nxn	d_s	*stdev*	*stdev*	*%*	*t_off*	*stdev*	*%*	*t_off*
3x3	1	472,63	18,25	96.1	8454,31	4,90	98.9	2643,55
	2	472,63	1,22	99.7	751,06	0,86	99.8	618,02
4x4	1	673,35	71,19	89.42	61356,88	22,02	96.7	21791,54
	2	673,35	12,02	98.2	14403,57	5,27	99.2	7168,65
	3	673,35	3,71	99.4	5659,23	3,11	99.5	5379,76
	4	673,35	3,20	99.5	5595,36	2,91	99.5	5757,87
6x6	1	768,79	172,30	77.5	223968,46	114,79	85.06	175384,77
	2	768,79	71,84	90.6	143341,99	31,26	95.9	71076,96
	3	768,79	14,77	98.1	38272,02	8,06	98.9	24275,51
	4	768,79	7,41	99.03	22071,98	6,39	99.1	22623,16
	5	768,79	8,34	98.9	26672,36	7,12	99.07	27619,37
	6	768,79	4,09	99.46	13140,15	3,88	99.4	15129,09
8x8	1	1054,37	277,27	73.7	612801,36	213,72	79.73	544451,70
	2	1054,37	152,70	85.51	533387,97	96,20	90.8	372905,83
	3	1054,37	62,39	94.08	287047,03	30,34	97.1	160189,13
	4	1054,37	23,53	97.7	129665,01	14,62	98.61	94582,26
	5	1054,37	11,21	98.9	72062,08	9,37	99.1	72118,55
	6	1054,37	10,47	99	74145,66	10,05	99.04	87118,93
	7	1054,37	11,73	98.88	87002,29	11,53	98.9	105536,68
	8	1054,37	14,33	98.6	105671,57	14,26	98.6	130574,54
11x11	1	1410,67	405,38	71.26	1566743,1	336,40	76.1	1468932,65
	2	1410,67	263,82	81.29	1650700,6	198,90	85.9	1357862,45
	3	1410,67	157,94	88.8	1273130,6	103,84	92.6	939250,97
	4	1410,67	90,06	92.61	872161,75	51,31	96.3	573573,45
	5	1410,67	47,06	96.6	546777,20	29,11	97.9	400616,91
	6	1410,67	27,13	98.07	368469,49	20,31	98.5	337224,70
	7	1410,67	19,63	98.6	300654,06	18,38	98.7	351409,98
	8	1410,67	19,11	98.6	317752,10	18,91	98.65	399305,73
	9	1410,67	25,03	98.2	421880,90	24,91	98.2	529532,55
	10	1410,67	24,62	98.25	444597,19	24,51	98.2	578157,20

Table D.2 Standard deviation, unbalance reduction percentage and trade-off between balance degree and time for torus topologies and for all possible d_s at different load-balancing steps for pathological initial load distributions